Are Ligand-Stabilized Carboxylic Acid Derivatives with Ge=Te Bonds Isolable?

Rahul Kumar Siwatch,[†] Dhirendra Yadav,[†] Goutam Mukherjee,[†] Gopalan Rajaraman,[‡] and Selvarajan Nagendran*,[†]

[†]Department of Chemistry, Indian Institute of Technology Delhi, Hauz Khas, New Delhi 110 016, India
[‡]Department of Chemistry, Indian Institute of Technology Bombay, Powai, Mumbai 400 076, India

Ⓢ Supporting Information

ABSTRACT: The stability of ligand-stabilized carboxylic acid derivatives (such as esters, amides, anhydrides, and acid halides) with terminal Ge=Te bonds is highly questionable as there is no report on such compounds. Nevertheless, we are able to isolate germatelluroester $[LGe(Te)Ot\text{-}Bu]$ (**4**), germatelluroamide $[LGe(Te)N(SiMe_3)_2]$ (**5**), and germatelluroacid anhydride $[LGe(Te)OGe(Te)L]$ (**6**) complexes (L = aminotroponiminate (ATI)) as stable species. Consequently, the synthetic details, structural characterization, and UV−vis spectroscopic and theoretical studies on them are reported for the first time.
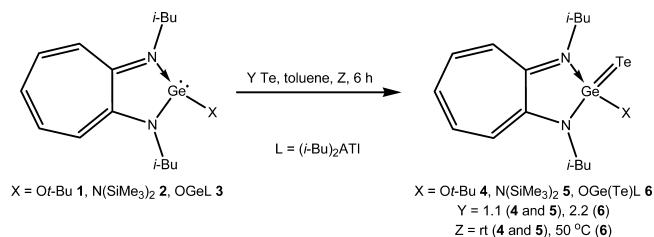

R = alkyl or aryl group; L = aminotroponiminate (ATI) ligand
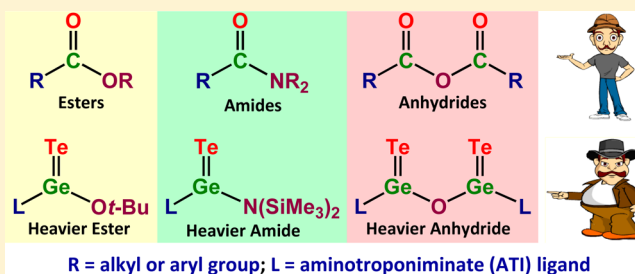
INTRODUCTION

Carboxylic acid derivatives $[RC(O)X]$ such as esters, amides, anhydrides, and acid halides (X = OR, NR_2, $OC(O)R$, and halogens, respectively) (R = alkyl or aryl group) have enormous importance in natural systems and synthetic organic chemistry.[1] In view of this significance, there have been continuous efforts to synthesize their heavier analogues (L′M(E)X) (L′ = a mono-anionic ligand/bulky aryl or alkyl group; M = Si, Ge, Sn; E = O, S, Se, Te) with multiple bonds between the heavier group 14 elements (M) and chalcogens (E).[2,3] However, the synthesis of such analogues is often challenged by the high polarity and/or weak π-orbital overlap in the M=E bonds,[2−4] especially when E is an oxygen[5] or a tellurium[6] atom. Thus, none of the afore-mentioned carboxylic acid derivatives with Ge=Te/O bonds are known.[2−6] This made us wonder whether compounds such as L′Ge(Te/O)X are isolable or not. To get an answer, we carried out a series of experiments and successfully isolated the first examples of germatelluroester, -amide, and -acid anhydride complexes. Accordingly, the synthesis of novel germatelluroester $[LGe(Te)Ot\text{-}Bu]$ (**4**), germatelluroamide $[LGe(Te)N(SiMe_3)_2]$ (**5**), and germatelluroacid anhydride $[LGe(Te)OGe(Te)L]$ (**6**) complexes (L = aminotroponiminate (ATI), a monoanionic bidentate ligand[3h−k,7]), their structural characterization, and UV−vis spectroscopic and theoretical studies are reported.

RESULTS AND DISCUSSION

Synthesis and Spectra. The reaction of ATI ligand-stabilized germylene alkoxide $[(i\text{-}Bu)_2ATIGeOt\text{-}Bu]$ (**1**),[3h] with 1.1 equiv of elemental tellurium in toluene at room temperature for 6 h, afforded the desired germatelluroester complex $[(i\text{-}Bu)_2ATIGe(Te)Ot\text{-}Bu]$ (**4**) in about 98% yield (Scheme 1). Similar reaction with germylene amide complex $[(i\text{-}Bu)_2ATIGeN(SiMe_3)_2]$ (**2**) [see the Experimental Section

Scheme 1. Synthesis of Germatelluroester (4), Germatelluroamide (5), and Germatelluroacid Anhydride (6) Complexes

L = (i-Bu)₂ATI

X = Ot-Bu **1**, N(SiMe₃)₂ **2**, OGeL **3**

X = Ot-Bu **4**, N(SiMe₃)₂ **5**, OGe(Te)L **6**
Y = 1.1 (**4** and **5**), 2.2 (**6**)
Z = rt (**4** and **5**), 50 °C (**6**)

(vide infra)] gave germatelluroamide complex $[(i\text{-}Bu)_2ATIGe(Te)N(SiMe_3)_2]$ (**5**) in 69% yield (Scheme 1). For the isolation of germatelluroacid anhydride complex $[\{(i\text{-}Bu)_2ATIGe(Te)\}_2O]$ (**6**) in about 65% yield, digermylene oxide complex $[\{(i\text{-}Bu)_2ATIGe\}_2O]$ (**3**)[3k] was reacted with 2.2 equiv of elemental tellurium in toluene at 50 °C for 6 h (Scheme 1). The other reaction conditions employed to obtain compounds **5** and **6** in high yields are not fruitful. The synthesis of compounds **4−6** represents the first successful oxidative addition of elemental tellurium on any germylene with OR, NR_2, and OGeL′ substituents.

Compounds **4−6** are red solids and are stable at room temperatures under an inert atmosphere for a few hours. However, if stored under low temperatures, no decomposition was observed. The attempts to isolate the oxygen analogues of compounds **4−6** were not successful until now. The reactions of compounds **1−3** with various oxygenating reagents, such as pyridine N-oxide,

nitrous oxide, trimethylamine *N*-oxide, and so forth, gave mixtures of unidentified products.

Compounds **4**–**6** have been characterized in solution by multinuclear NMR spectroscopy (^{1}H, ^{13}C, ^{29}Si, and ^{125}Te). In the ^{1}H NMR spectrum of compound **4**, the protons of methyl and methylene groups appear as two doublets that are overlapping with each other (0.89–0.93 ppm) and two double doublets (3.32, and 3.66 ppm) due to diastereotopicity, respectively.[3h−k] A singlet (1.73 ppm) and multiplet (2.32–2.46 ppm) resonances were observed for the *t*-butoxide and methine protons. As expected, the five protons of the seven-membered ring appeared as a triplet (6.16 ppm), doublet (6.35 ppm), and pseudotriplet (6.62 ppm). This splitting pattern is also seen for the seven-membered ring protons in compounds **5** and **6** between 6.16 and 6.69 ppm. In compound **5**, the methyl, methine, and methylene protons of *i*-butyl substituents appear as a pseudotriplet (due to the merging of two doublets) (0.95 ppm), a multiplet (2.60–2.74 ppm), and two double doublets (3.29, 3.72 ppm), respectively. A singlet resonance at 0.48 ppm confirms the presence of trimethylsilyl groups. In contrast to compounds **4** and **5**, the two doublet resonances for the methyl protons of the *i*-butyl groups in compound **6** are well separated (0.85 and 0.98 ppm), and the methine (2.40–2.49 ppm) and methylene (3.72–3.86 ppm) protons of the same groups appear as multiplets. Ten, nine, and eight signals anticipated for compounds **4**, **5**, and **6** in their ^{13}C NMR spectra were seen, respectively.[3h−k] The additional two and one signals in compounds **4** and **5** in comparison to compound **6** are due to the carbon atoms of *t*-butoxide and trimethylsilyl groups, respectively. A sharp signal (−0.47 ppm) in the ^{29}Si NMR spectrum of compound **5** substantiates the presence of trimethylsilyl groups. In the ^{125}Te NMR spectra of compounds **4**, **5**, and **6**, the signals at −791.20, −584.60, and −884.09 ppm confirm the presence of tellurium atoms in them, respectively. As germatelluro carboxylic acid derivatives are unknown,[2−4,6] for comparison, germatelluroketones[6c,d] **I**–**III** (Chart 1) are used. The resonances for the

Chart 1. Structures of Compounds I−IV
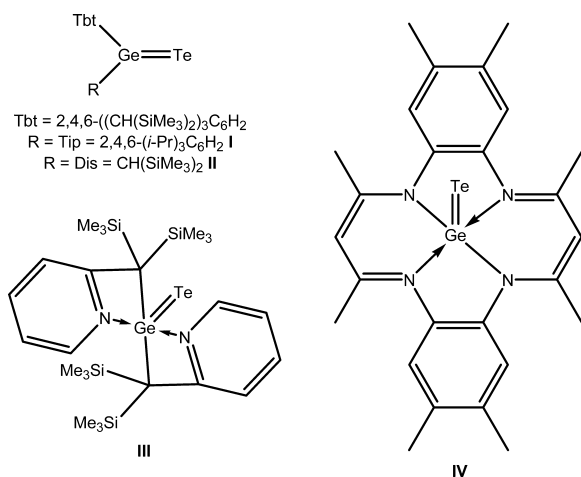
tellurium atoms are extremely upfield shifted against the same resonances in Okazaki's electronically unperturbed germaketones ([Tbt(Tip)Ge=Te] (**I**) (1143 ppm) and [Tbt(Dis)Ge=Te] (**II**) (1009 ppm)) with tricoordinate germanium atoms (Chart 1).[6c] Even they are appreciably upfield shifted as compared to that seen in an electronically perturbed germaketone ([{2-(C(SiMe$_3$)$_2$)C$_5$H$_4$N}$_2$Ge=Te] (**III**) (−460.93 ppm))

with pentacoordinate germanium atom (Chart 1).[6d] This is attributable to the difference in the coordination environment around the germanium atoms in compounds **4**–**6**. In the UV–vis spectroscopic studies, compounds **4**–**6** show an absorption maxima in the visible region (Figure 1). On the basis of
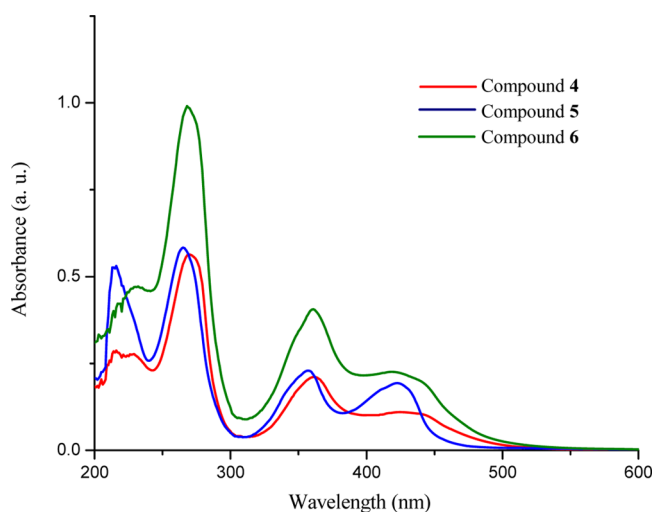

Figure 1. UV−vis spectra of compounds **4**−**6** (15.8 μM solution) in tetrahydrofuran.

theoretical studies, it is predicted that the origin of these peaks is due to the $\pi_{(Ge=Te)} \rightarrow \pi^*_{(ATI)}$ electronic transitions (Table 1). Nevertheless, it should be noted that the $\pi_{(Ge=Te)}$ bonds in these compounds are highly polarized toward tellurium atoms (*vide infra*). Apart from this, all of these compounds in common show two intense peaks around 360 and 270 nm (Figure 1). While the former peaks are mainly due to the $\pi_{(ATI)} \rightarrow \pi^*_{(ATI)}$ electronic transitions, the latter peaks are due to multiple transitions (Table 1). Interestingly, the kinetically stabilized germaketones **I** and **II** show absorption maxima at 636 and 599 nm due to n $\rightarrow$ π^* transitions of the Ge=Te bonds,[6c] respectively.

X-ray Crystal Structures of Compounds 4-6. Single crystals of compounds **4**−**6** suitable for the X-ray diffraction analysis were grown by cooling their solutions [for details, see the Experimental Section] at −40 °C. Compounds **4**, **5**, and **6** crystallized in the monoclinic space groups $P2_1/c$, $P2_1/n$, and $P2_1/n$, with one, one, and two molecules in the asymmetric unit cell, respectively. All these compounds are monomeric in the solid state, and there is no intermolecular Ge⋯Te interaction up to 5 Å. The molecular structure of compound **4** shows the germaester moiety [(Te)GeO*t*-Bu] along with the aminotroponiminate ligand (Figure 2). The germanium atom is tetracoordinate with a distorted tetrahedral geometry and has an immediate environment of a tellurium, an oxygen, and two nitrogen atoms (Figure 2).

The lengths of the Ge−O and Ge−N bonds in compound **4** are 1.771(3) and 1.886 Å (average), respectively, and these values are comparable to those found in germathio- (Ge−O 1.765(4) Å and Ge−N 1.879 Å (average)) and germaselenoester (Ge−O 1.774(3) Å and Ge−N 1.888 Å (average)) complexes [(*i*-Bu)$_2$ATIGe(E)O*t*-Bu] (E = S, Se).[3h] The Ge=Te bond length (2.4374(4) Å) in compound **4** is in between the corresponding bond lengths in the electronically unperturbed (**I** (2.398(1) Å) and **II** (2.384(2) Å))[6c] and perturbed (**III** (2.4795(5) Å)[6d] and **IV** [{η^4-Me$_8$taa}Ge=Te] (2.466(1) Å))[6a]

Table 1. Observed and Calculated UV−Vis Absorption Maxima of Compounds 4−6^a

transition	origin of transition (percentage contribution)	λ_{max} (ε) obsd	λ_{max} (f) calcd
	Compound 4		
$\pi_{(Ge=Te)} \rightarrow \pi^*_{(ATI)}$	HOMO−1 → LUMO (6)	424 (6956)	419.62 (0.0374)
$\pi_{(Ge=Te)} \rightarrow \pi^*_{(ATI)}$	HOMO → LUMO+1 (90)		
$a_{(1)} + \pi_{(ATI)} \rightarrow \pi^*_{(ATI)}$	HOMO−3 → LUMO (9)	362 (13 323)	331.40 (0.2471)
$\pi_{(ATI)} \rightarrow \pi^*_{(ATI)}$	HOMO−2 → LUMO+1 (86)		
$a_{(1)} + \pi_{(ATI)} \rightarrow \pi^*_{(ATI)}$	HOMO−5 → LUMO+1 (34)	270 (35 652)	240.90 (0.4352)
$a_{(1)} + \sigma_{(Ge-Te)} \rightarrow \pi^*_{(ATI)}$	HOMO−4 → LUMO (19)		
$a_{(1)} + \pi_{(ATI)} \rightarrow \pi^*_{(ATI)}$	HOMO−3 → LUMO (14)		
$\pi_{(ATI)} \rightarrow \pi^*_{(ATI)}$	HOMO−2 → LUMO+1 (3)		
$\pi_{(Ge=Te)} \rightarrow \pi^*_{(Ge=Te)}$	HOMO−1 → LUMO+3 (27)		
	Compound 5		
$\pi_{(Ge=Te)} \rightarrow \pi^*_{(ATI)}$	HOMO−1 → LUMO (23)	422 (12 234)	441.85 (0.0447)
$\pi_{(Ge=Te)} \rightarrow \pi^*_{(ATI)}$	HOMO → LUMO+1 (73)		
$\pi_{(ATI)} \rightarrow \pi^*_{(ATI)}$	HOMO−4 → LUMO (9)	357 (14 506)	338.20 (0.2546)
$\pi_{(ATI)} \rightarrow \pi^*_{(ATI)}$	HOMO−2 → LUMO+1 (87)		
$a_{(2)} + \sigma_{(Ge-Te)} \rightarrow \pi^*_{(ATI)}$	HOMO−5 → LUMO+1 (7)	265 (36 911)	243.30 (0.5996)
$\pi_{(ATI)} \rightarrow \pi^*_{(ATI)}$	HOMO−4 → LUMO (59)		
$\pi_{(ATI)} \rightarrow \pi^*_{(ATI)}$	HOMO−2 → LUMO+1 (6)		
$\pi_{(Ge=Te)} \rightarrow \pi^*_{(Ge=Te)}$	HOMO−1 → LUMO+3 (18)		
	Compound 6		
$\pi_{(Ge=Te)} \rightarrow \pi^*_{(ATI)}$	HOMO−1 → LUMO (25)	419 (14 272)	416.65 (0.0369)
$\pi_{(Ge=Te)} \rightarrow \pi^*_{(ATI)}$	HOMO −1 → LUMO+2 (42)		
$\pi_{(Ge=Te)} \rightarrow \pi^*_{(ATI)}$	HOMO → LUMO+1 (19)		
$\pi_{(Ge=Te)} \rightarrow \pi^*_{(ATI)}$	HOMO → LUMO+3 (12)		
$\pi_{(ATI)} \rightarrow \pi^*_{(ATI)}$	HOMO−4 → LUMO+2 (93)	361 (25 671)	348.00 (0.2246)
$\pi_{(ATI)} \rightarrow \pi^*_{(ATI)}$	HOMO−7 → LUMO (35)	268 (62 722)	245.16 (0.8792)
$\pi_{(ATI)} \rightarrow \pi^*_{(ATI)}$	HOMO−6 → LUMO+1 (40)		
$\pi_{(ATI)} \rightarrow \pi^*_{(ATI)}$	HOMO−5 → LUMO+2 (4)		
$\pi_{(ATI)} \rightarrow \pi^*_{(ATI)}$	HOMO−4 → LUMO+3 (5)		
$\pi_{(Ge=Te)} \rightarrow \pi^*_{(Ge=Te)}$	HOMO−3 → LUMO+6 (2)		

$^a a_{(1)} = nb_{(O)} + \sigma_{(C-C)} + \sigma_{(C-H)}$ and $a_{(2)} = \sigma_{(Si-C)} + \sigma_{(C-H)} + \sigma_{(Si-N)}$.

germaketones (Me$_8$taa = octamethyldibenzo-tetraaza[14]annulene) (Chart 1). This is probably due to the high and low electronic perturbation in compound **4** as compared to those in compounds **I−II** and **III−IV**, respectively.

Molecular structures of compounds **5** (Figure 3) and **6** (Figure 4) confirm the formation of ligand-stabilized germaamide and germaacid anhydride with $[(Te)GeN(SiMe_3)_2]$ and $[(Te)GeOGe(Te)]$ moieties, respectively. The germanium(IV) atoms in these compounds are also tetracoordinate and possess a distorted tetrahedral geometry. The coordination environments around them contain one tellurium and three nitrogen atoms in compound **5** and one tellurium, two nitrogen, and one oxygen atoms in compound **6**. The average Ge−N$_{(ligand)}$ bond lengths in compounds **5** (1.900 Å) and **6** (1.888 Å) are reminiscent of the situation in compound **4**. The Ge−N$_{(amide)}$ bond (1.851(3) Å) in compound **5** is slightly shorter than the Ge−N$_{(ligand)}$ bonds in compounds **4−6**.

An indication of the increased oxidation state (from +2 to +4) of the germanium atoms upon telluration can be realized through the marginally reduced lengths of the Ge−O bonds in compounds **6** (1.765 Å (average)) against the lengths of the same bonds in its precursor (compound **3**; 1.791 Å (average)).[3k] The

average Ge−O−Ge bond angle in compound **6** (134.7°) is considerably less than the Ge−O−Ge bond angle (154.9(3)°) found in compound **3**.[3k] The lengths of the Ge=Te and average Ge=Te bonds in compounds **5** (2.4450(5) Å) and **6** (2.428 Å) follow the trend seen in compound **4** (vide supra), respectively. Further, the Ge=Te bond lengths in these compounds (**4−6**) are shorter and longer than the sum of the single (2.59 Å) and double (2.39 Å) bond covalent radii of germanium and tellurium atoms, respectively.[6a,8] Therefore, the Ge=Te bonds in these compounds (**4−6**) can be considered to have a polar nature somewhere in between the two extreme forms Ge=Te and Ge$^+$−Te$^-$.[2−6]

Theoretical Studies on Compounds 4−6. To shed more light into the nature of the polar Ge=Te bonds in compounds **4−6**, DFT calculations were carried out using the GAUSSIAN 09 programs.[9] Further, how the Ge=Te bonds are affected by the substituents, such as −Ot-Bu, −N(SiMe$_3$)$_2$, and −OGe(Te)L, attached to the germanium atoms in compounds **4**, **5**, and **6**, was also probed, respectively. The NBO analysis[10,11] reveals that the bond ionicity (i_{Ge-Te}) in compound **5** is 0.070 with 53.50% and 46.50% donation from the germanium and tellurium atoms, respectively. The ionicities (i_{Ge-Te}) of the Ge−Te bonds in
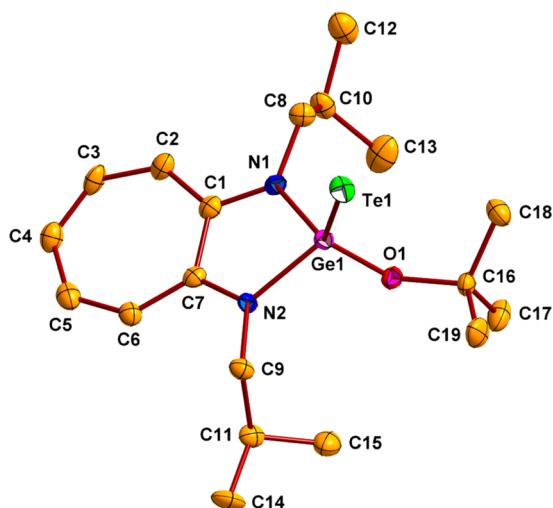
Figure 2. Molecular structure of germatelluroester complex **4**. Thermal ellipsoids are drawn at the 40% probability level. All the hydrogen atoms are omitted for clarity. Important bond lengths (Å) and angles (deg): Ge1−Te1 2.4374(4), Ge1−O1 1.771(3), Ge1−N1 1.878(3), Ge1−N2 1.893(3); Te1−Ge1−O1 123.67(8), Te1−Ge1−N1 117.74(9), Te1−Ge1−N2 118.50(9), O1−Ge1−N1 102.2(1), O1−Ge1−N2 103.0(1), N1−Ge1−N2 83.7(1).
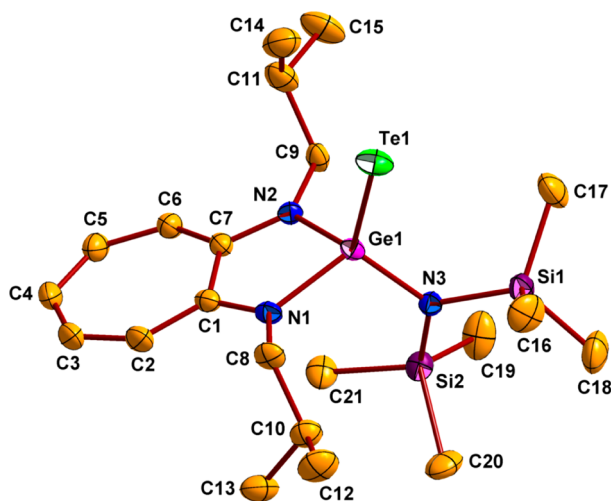

Figure 3. Molecular structure of germatelluroamide complex **5**. Thermal ellipsoids are drawn at the 40% probability level. All the hydrogen atoms are omitted for clarity. Important bond lengths (Å) and angles (deg): Ge1−Te1 2.4450(5), Ge1−N3 1.851(3), Ge1−N1 1.902(3), Ge1−N2 1.897(3); Te1−Ge1−N3 121.5(1), Te1−Ge1−N1 110.1(1), Te1−Ge1−N2 116.4(1), N3−Ge1−N1 111.0(2), N3−Ge1−N2 107.7(2), N1−Ge1−N2 83.9(1).

compounds **4** (0.073) and **6** (0.065) are very similar as compared to that seen in compound **5**. Accordingly, the contributions of the germanium (**4** 53.63%, **6** 53.23%) and tellurium (**4** 46.37% and **6** 46.77%) atoms are also quite comparable. Further, in compound **5**, the Ge−Te σ−bond is formed by the overlap of sp$^{0.61}$ hybridized orbital of germanium and sp$^{9.18}$ hybridized orbital of tellurium. Similar hybridizations of the germanium and tellurium atoms are observed for compounds **4** and **6**. The NBO analysis (on the basis of second order perturbation theory) on compound **5** shows three major interactions between tellurium and germanium atoms (Figure 5d−f). Among these, the π-antibonding interaction between the p-orbitals of tellurium and germanium atoms gave a maximum stabilization of 32 kcal/mol
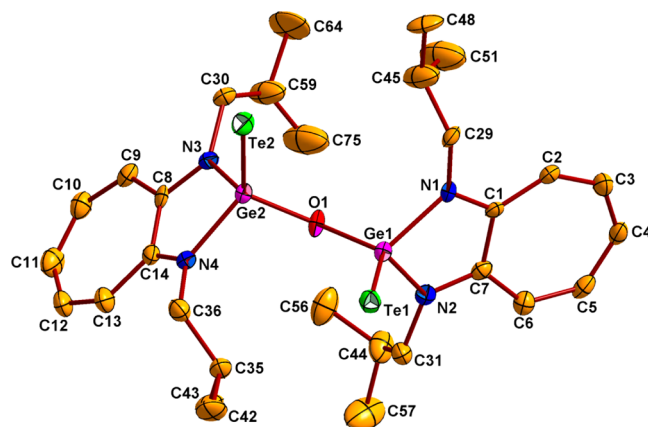

Figure 4. Molecular structure of germatelluroacid anhydride complex **6**. Thermal ellipsoids are drawn at the 30% probability level. All hydrogen atoms are omitted for clarity; further, one of the two molecules and a tetrahydrofuran molecule present in the asymmetric unit cell are not shown. Important bond lengths (Å) and angles (deg): Ge1−Te1 2.434(1) {2.435(1)}, Ge2−Te2 2.426(1) {2.415(1)}, Ge1−O1 1.766(5) {1.758(5)}, Ge2−O1 1.762(5) {1.772(5)}, Ge1−N1 1.896(6) {1.874(6)}, Ge1−N2 1.876(6) {1.888(7)}, Ge2−N3 1.886(6) {1.894(6)}, Ge2−N4 1.892(6) {1.890(6)}; Te1−Ge1−O1 119.6(2) {120.6(2)}, Te2−Ge2−O1 117.7(2) {118.8(2)}, Ge1−O1−Ge2 133.2(3) {136.1(3)}, Te1−Ge1−N1 117.7(2) {119.0(2)}, Te1−Ge1−N2 119.6(2) {118.2(2)}, Te2−Ge2−N3 116.2(2) {113.4(2)}, Te2−Ge2−N4 124.3(2) {127.2(2)}, O1−Ge1−N1 108.1(3) {102.2(3)}, O1−Ge1−N2 101.3(2) {106.0(3)}, O1−Ge2−N3 103.3(3) {104.0(3)}, O1−Ge2−N4 104.8(3) {102.3(3)}, N1−Ge1−N2 84.3(3) {84.1(3)}, N3−Ge2−N4 84.4(3) {84.2(3)}. The values given in the braces { } represent the corresponding bond lengths/angles in the other molecule.

to the Ge=Te bond (Figure 5f). The other two stabilizing interactions are σ- (15 kcal/mol) and π- (28 kcal/mol) bonding overlap between the tellurium and germanium atoms (Figures 5d and 5e, respectively). In contrast, compounds **4** and **6** have two significant π-antibonding and one σ-bonding interactions between tellurium and germanium atoms (Figures 5a−c and 5g−i).

Additionally, in compound **5**, there is a significant donation from the nitrogen atom of the N(SiMe$_3$)$_2$ group to the Ge−Te antibonding orbital, and this donation yields a stabilization of 10 kcal/mol to the system (Figure 6b). However, in compounds **4** and **6** the stabilization energies due to the donation of lone pairs of oxygen atoms to the antibonding Ge−Te orbitals are 6 and 8 kcal/mol, respectively (Figures 6a and 6c).

These discussions clearly suggest the polarization in the Ge=Te bonds in compounds **4−6** and corroborate the prediction based on the Ge=Te bond lengths from the solid-state structural analysis. This finding is further substantiated by the NPA charge analysis and WBI calculations on compounds **4−6** (Supporting Information Table S4). To ascertain the contributions of the two extreme resonating forms, Ge=Te and Ge$^+$−Te$^−$, to the Ge=Te bond, NRT analysis[12] was performed on compound **4**, which suggests that the weightages of the forms Ge=Te and Ge$^+$−Te$^−$ are 48% and 52%, respectively. Molecular orbital calculations on these compounds (**4**, **5**, and **6**) also confirm the presence of orbital overlaps between tellurium and germanium atoms along the Ge−Te bond axes at the HOMO−4, HOMO−5, and HOMO−8 energy levels (Supporting Information Figure S1a, b, and c, respectively). The HOMOs are predominantly centered on the tellurium atoms and are π-bonding between germanium and tellurium atoms (see
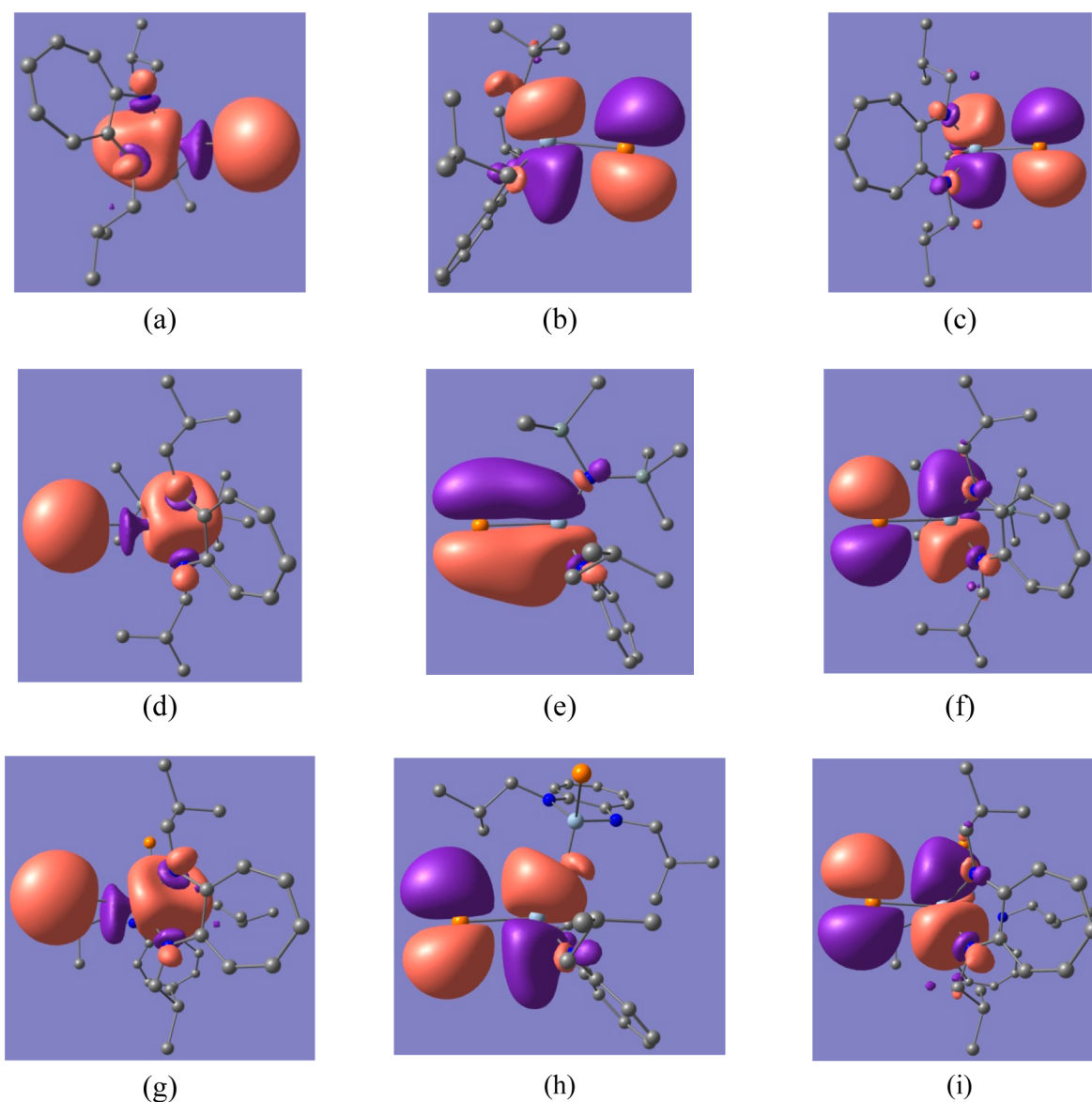
Figure 5. NBO computed orbital interactions (from the second order perturbation theory analysis) in the Ge═Te bonds in compounds **4** (a−c), **5** (d−f), and **6** (g−i). The σ-interactions in these compounds is due to the overlap between sp^x (x = 2.15 **4**, 1.67 **5**, and 2.33 **6**) hybrid orbitals of germanium atoms and s-orbitals (predominantly) of tellurium atoms, whereas the π-bonding and π-antibonding interactions are formed by the overlap of p-orbitals of germanium and tellurium atoms.
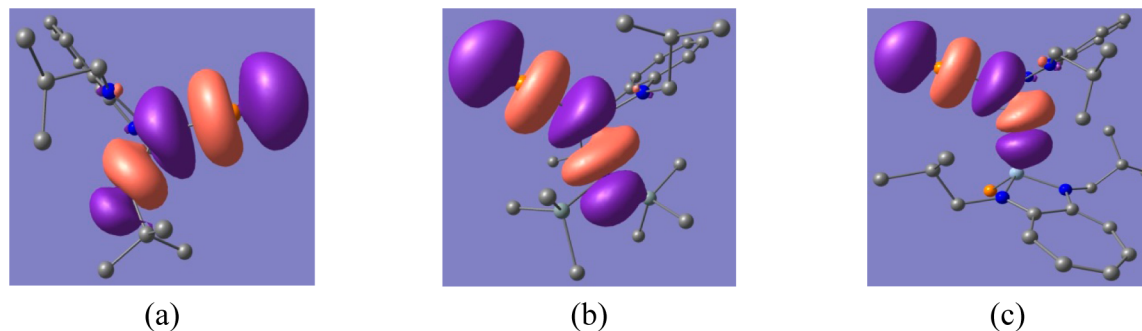

Figure 6. Interaction of the lone pairs on oxygen (of −Ot-Bu), nitrogen (of −N(SiMe$_3$)$_2$), and oxygen (of −OGe(Te)L) atoms with the Ge−Te antibonding orbitals in compounds **4** (a), **5** (b), and **6** (c), respectively.

Supporting Information Figure S2). This may be associated with the electronegativity difference and the fact that the valence 5p-orbitals in tellurium are more diffused than the valence 4p-

orbitals of germanium. The LUMOs are mainly composed of the π-antibonding orbitals of the fused rings (Supporting Information Figure S2).

CONCLUSIONS

In brief, we have reported the first ligand-stabilized carboxylic acid derivatives such as ester (**4**), amide (**5**), and anhydride (**6**) complexes with formal Ge═Te bonds. These compounds were obtained through the oxidative addition of elemental tellurium to the germylene complexes **1**−**3** with tricoordinate germanium atoms. Interestingly, complexes **4**−**6** are the first examples of germanium compounds with tetracoordinate germanium atoms and Ge═Te bonds. The hint of polarized Ge═Te double bonds given by the solid-state structures of these compounds has been proven by DFT calculations. The NBO analysis reveals that the polarization is due to the stabilizing π-antibonding interactions between germanium and tellurium atoms and the donation of electrons by the N/O atom of the substituent to the Ge−Te antibonding orbital.

EXPERIMENTAL SECTION

All the reactions and handling of air and moisture sensitive compounds were performed under an inert atmosphere of dry nitrogen gas by means of the standard Schlenk and/or glovebox techniques. The solvents used for the synthesis were dried according to the standard procedures. Benzene-d_6 for NMR spectroscopic studies was dried over potassium mirror. Germylene alkoxide [(*i*-Bu)$_2$ATIGeO*t*-Bu] (**1**)[3h] and digermylene oxide [{(*i*-Bu)$_2$ATIGe}$_2$O] (**3**)[3k] complexes were prepared according to the literature procedures. Germylene amide [(*i*-Bu)$_2$ATIGeN-(SiMe$_3$)$_2$] (**2**) complex was synthesized through the reaction of aminotroponiminatogermylene monochloride [(*i*-Bu)$_2$ATIGeCl] with LiN(SiMe$_3$)$_2$. Details regarding this synthesis will be published elsewhere.[13] Elemental tellurium was purchased from Aldrich and used as such without any further purification. Melting points of the new compounds were measured using an Ambassador melting point apparatus, and the reported values are uncorrected. Elemental analysis was performed using a Perkin-Elmer CHN analyzer. Multinuclear NMR (^{1}H, ^{13}C, ^{29}Si, and ^{125}Te) spectroscopic studies were carried out on a 300 MHz Bruker Topsin NMR spectrometer. The reported values of chemical shifts δ are in ppm. The referencing was done internally with respect to the residual solvent and solvent resonances in the case of ^{1}H and ^{13}C NMR spectra, respectively.[14] For the ^{29}Si and ^{125}Te NMR spectroscopic studies, tetramethylsilane and dimethyl telluride were used as the external references, respectively. UV−vis absorption spectra of compounds **4**−**6** were recorded on a SHIMADZU-UV-2450 UV−vis spectrophotometer at room temperatures using a screw-cap cuvette.

Synthesis of [(*i*-Bu)$_2$ATIGe(Te)O*t*-Bu] (4). To a solution of compound **1** (0.58 g, 1.54 mmol) in toluene (10 mL) was added elemental tellurium (0.22 g, 1.69 mmol) at room temperature, and the reaction mixture stirred for 6 h. After that, the reaction mixture was filtered through a G4 frit (with Celite), and the solvent from the filtrate was removed under reduced pressure to afford a red residue. It was washed with hexane (5 mL) and dried *in vacuo* to get an analytically pure sample of compound **4** as a red solid. Single crystals of compound **4** were grown by cooling its toluene solution at −40 °C. Yield: 0.76 g, (1.51 mmol), 98%. Mp: 112 °C (dec). Anal. Calcd for C$_{19}$H$_{32}$GeN$_2$OTe (M = 504.71): C, 45.21; H, 6.39; N, 5.55. Found: C, 45.17; H, 6.44; N, 5.61. ^{1}H NMR (300 MHz, C$_6$D$_6$): δ 0.90 (d, $^3J_{HH}$ = 6.6 Hz, 6H, CH(CH_3)$_2$), 0.92 (d, $^3J_{HH}$ = 6.3 Hz, 6H, CH(CH_3)$_2$), 1.73 (s, 9H, C(CH_3)$_3$), 2.32−2.46 (m, 2H, CH(CH$_3$)$_2$), 3.32 (dd, J_{HH} = 13.8, 6.6 Hz, 2H, CH_2), 3.66 (dd, J_{HH} = 14.1, 6.3 Hz, 2H, CH_2), 6.16 (t, $^3J_{HH}$ = 9.0 Hz, 1H, CH), 6.35 (d, $^3J_{HH}$ = 11.1 Hz, 2H, CH), 6.62 (t, $^3J_{HH}$ = 9.9 Hz, 2H, CH). ^{13}C{^{1}H} NMR (75.48 MHz, C$_6$D$_6$): δ 21.10 (CH(CH$_3$)$_2$), 21.21 (CH(CH$_3$)$_2$), 27.85 (CH(CH$_3$)$_2$), 33.50 (C(CH$_3$)$_3$), 53.06 (CH_2), 75.57 (C(CH$_3$)$_3$), 116.30 (C$_4$), 124.48 (C$_{2,6}$), 137.37 (C$_{3,5}$), 156.32 (C$_{1,7}$). ^{125}Te{^{1}H} NMR (94.62 MHz, C$_6$D$_6$): δ −791.20 (Ge═*Te*). UV−vis (THF) λ_{max}/nm (ε/M^{-1} cm^{-1}): 270 (35 652), 362 (13 323), 424 (6956).

Synthesis of [(*i*-Bu)$_2$ATIGe(Te)N(SiMe$_3$)$_2$] (5). To a solution of compound **2** (0.51 g, 1.10 mmol) in toluene (10 mL) was added elemental tellurium (0.15 g, 1.21 mmol) at room temperature, and the reaction mixture stirred for 6 h. This mixture was filtered through a G4

frit (with Celite), and the solvent from the filtrate was removed under reduced pressure to afford a red residue. It was washed with hexane (5 mL) and dried *in vacuo* to get an analytically pure sample of compound **5** as a red solid. Single crystals of compound **5** were grown by cooling its toluene solution at −40 °C. Yield: 0.45 g, (0.76 mmol), 69%. Mp: 125 °C (dec). Anal. Calcd for C$_{21}$H$_{41}$GeN$_3$Si$_2$Te (M = 591.98): C, 42.61; H, 6.98; N, 7.10. Found: C, 42.65; H, 7.03; N, 7.12. ^{1}H NMR (300 MHz, C$_6$D$_6$): δ 0.48 (s, 18H, Si(CH_3)$_2$), 0.94 (d, $^3J_{HH}$ = 6.0 Hz, 6H, CH(CH_3)$_2$), 0.96 (d, $^3J_{HH}$ = 6.3 Hz, 6H, CH(CH_3)$_2$), 2.60−2.74 (m, 2H, CH(CH$_3$)$_2$), 3.29 (dd, J_{HH} = 13.8, 6.9 Hz, 2H, CH_2), 3.72 (dd, J_{HH} = 13.8, 6.6 Hz, 2H, CH_2), 6.16 (t, $^3J_{HH}$ = 9.6 Hz, 1H, CH), 6.38 (d, $^3J_{HH}$ = 11.1 Hz, 2H, CH), 6.68 (t, $^3J_{HH}$ = 10.2 Hz, 2H, CH). ^{13}C{^{1}H} NMR (75.48 MHz, C$_6$D$_6$): δ 6.88 (Si(CH$_3$)$_2$), 21.64 (CH(CH$_3$)$_2$), 22.07 (CH(CH$_3$)$_2$), 29.17 (CH(CH$_3$)$_2$), 54.05 (CH_2), 117.14 (C$_4$), 124.85 (C$_{2,6}$), 137.84 (C$_{3,5}$), 156.85 (C$_{1,7}$). ^{29}Si{^{1}H} NMR (59.63 MHz, C$_6$D$_6$): δ −0.47 (*Si*(CH$_3$)$_3$). ^{125}Te{^{1}H} NMR (94.62 MHz, C$_6$D$_6$): δ −584.60 (Ge═*Te*). UV−vis (THF) λ_{max}/nm (ε/M^{-1} cm^{-1}): 213 (33 323), 265 (36 911), 357 (14 506), 422 (12234).

Synthesis of [{(*i*-Bu)$_2$ATIGe(Te)}$_2$O] (6). To a solution of compound **3** (0.51 g, 0.82 mmol) in toluene (40 mL) was added elemental tellurium (0.23 g, 1.80 mmol) at room temperature, and this mixture was heated with stirring at 50 °C for 6 h. This mixture was filtered through a G4 frit (with Celite), and the solvent from the filtrate was removed under reduced pressure to afford a red residue. It was washed with hexane (7 mL) and dried *in vacuo* to get an analytically pure sample of compound **6** as a red solid. Single crystals of compound **6** were grown by cooling its THF solution at −40 °C. Yield: 0.47 g, (0.54 mmol), 65%. Mp: 96 °C (dec). Anal. Calcd for C$_{30}$H$_{46}$Ge$_2$N$_4$OTe$_2$ (M = 879.19): C, 40.98; H, 5.27; N, 6.37. Found: C, 40.96; H, 5.31; N, 6.43. ^{1}H NMR (300 MHz, C$_6$D$_6$): δ 0.85 (d, $^3J_{HH}$ = 6.3 Hz, 12H, CH(CH_3)$_2$), 0.98 (d, $^3J_{HH}$ = 6.6 Hz, 12H, CH(CH_3)$_2$), 2.40−2.49 (m, 4H, CH(CH$_3$)$_2$), 3.72−3.86 (m, 8H, CH_2), 6.22 (t, $^3J_{HH}$ = 9.3 Hz, 2H, CH), 6.53 (d, $^3J_{HH}$ = 11.1 Hz, 4H, CH), 6.69 (t, $^3J_{HH}$ = 10.5 Hz, 4H, CH). ^{13}C{^{1}H} NMR (75.48 MHz, C$_6$D$_6$): δ 20.91 (CH(CH$_3$)$_2$), 21.34 (CH(CH$_3$)$_2$), 28.28 (CH(CH$_3$)$_2$), 53.74 (CH_2), 115.95 (C$_4$), 124.01 (C$_{2,6}$), 137.21 (C$_{3,5}$), 157.12 (C$_{1,7}$). ^{125}Te{^{1}H} NMR (94.62 MHz, C$_6$D$_6$): δ −884.09 (Ge═*Te*). UV−vis (THF) λ_{max}/nm (ε/M^{-1} cm^{-1}) 268 (62 722), 361 (25 671), 419 (14 272).

X-ray Structure Determination for Compounds 4−6. The X-ray data for compounds **4**−**6** were collected using a Bruker SMART APEX diffractometer equipped with a 3-axis goniometer at 100 K.[15] The crystals were mounted on a glass fiber after covering them with a cryoprotectant. SAINT and SADABS were used to integrate the data and apply an empirical absorption correction, respectively.[16] SHELXTL was used for structural solution by direct methods and refinement by full-matrix least-squares on F^2.[17] Anisotropic refinement was performed for all the non-hydrogen atoms. A riding model was used to fix the positions of the hydrogen atoms, and they were refined isotropically. The crystallographic data for these compounds (**4**−**6**) are given in Supporting Information Table S1. For compound **6**, among the four tetrahydrofuran molecules that were present in the crystal lattice, three were highly disordered. The disordered molecules were removed using Platon/Squeeze program.[18]

Computational Details. GAUSSIAN-09 programs were used for carrying out all the calculations.[9] The B3LYP level of theory was used for optimizing the geometries of compounds **4**−**6** using a LANL2DZ (having ECP for core electrons) (for tellurium, germanium, and silicon atoms), 6-311+G* (for nitrogen and oxygen atoms), and 3-21G* (for carbon and hydrogen atoms) basis sets. For geometry optimizations, the coordinates obtained from single crystal X-ray diffraction studies were used. The frequency calculations were carried out for all the optimized geometries of compounds **4**−**6** to characterize the stationary points as minima. The same level of theory and the optimized coordinates were used for performing the Weinhold's natural bond orbital (NBO),[10,11] NPA charges and orbital populations, and WBI analyses on these compounds. Chemcraft software (http://www.chemcraftprog.com) was used for plotting the NBO interactions. The computed bond lengths and angles match well with the experimentally obtained values except for the Ge−O−Ge bond angle in compound **6** (which may be attributed to the lattice effects[3k]) (Supporting Information Tables S2

and S3). NRT analysis was performed using NBO 5.0 software. To explain the UV–vis spectra of compounds **4–6**, TDDFT-PCM calculations were carried out using tetrahydrofuran as solvent. B3LYP level of theory and the optimized coordinates were used. The basis set used is SDD (having ECP for core electrons) for tellurium, germanium, and silicon atoms. For other atoms, the aforementioned basis sets were used.

■ ASSOCIATED CONTENT

Ⓢ Supporting Information

Crystallographic information file (CIF) for compounds **4–6**, crystal data and structure refinement parameters for compounds **4–6** (Table S1), MOs of compounds **4–6** that show the σ-bonds between the tellurium and germanium atoms (Figure S1), FMOs of compounds **4–6** (Figure S2), selected bond lengths and angles of compounds **4–6** obtained from calculations (Table S2 and S3, respectively), Wiberg bond indices and NPA charges of the atoms connected to the germanium atoms in compounds **4–6** (Table S4), and complete author list for ref 9. This material is available free of charge via the Internet at http://pubs.acs.org.

■ AUTHOR INFORMATION

Corresponding Author

*E-mail: sisn@chemistry.iitd.ac.in.

Notes

The authors declare no competing financial interest.

■ ACKNOWLEDGMENTS

■ REFERENCES

(1) (a) Carey, F. A.; Sundberg, R. J. *Advanced Organic Chemistry, Part B: Reactions and Synthesis*, 5th ed.; Springer Science+Business Media: New York, 2007. (b) Vollhardt, K.; Peter, C. *Organic Chemistry: Structure and Function*, 6th ed.; W. H. Freeman and Company: New York, 2011.

(2) (a) Barrau, J.; Rima, G. *Coord. Chem. Rev.* **1998**, *178–180*, 593. (b) Tokitoh, N.; Okazaki, R. *Coord. Chem. Rev.* **2000**, *210*, 251. (c) Bourget-Merle, L.; Lappert, M. F.; Severn, J. R. *Chem. Rev.* **2002**, *102*, 3031. (d) Kühl, O. *Coord. Chem. Rev.* **2004**, *248*, 411. (e) Saur, I.; Alonso, S. G.; Barrau, J. *Appl. Organomet. Chem.* **2005**, *19*, 414. (f) Leung, W.-P.; Kan, K.-W.; Chong, K.-H. *Coord. Chem. Rev.* **2007**, *251*, 2253. (g) Nagendran, S.; Roesky, H. W. *Organometallics* **2008**, *27*, 457. (h) Mizuhata, Y.; Sasamori, T.; Tokitoh, N. *Chem. Rev.* **2009**, *109*, 3479. (i) Mandal, S. K.; Roesky, H. W. *Chem. Commun.* **2010**, *46*, 6016. (j) Lee, V. Y.; Sekiguchi, A. *Organometallic Compounds of Low-Coordinate Si, Ge, Sn, and Pb: From Phantom Species to Stable Compounds*; Wiley: Chichester, U.K., 2010. (k) Asay, M.; Jones, C.; Driess, M. *Chem.*

Rev. **2011**, *111*, 354. For examples that are not covered in these reviews see ref 3.

(3) (a) Hitchcock, P. B.; Hu, J.; Lappert, M. F.; Severn, J. R. *Dalton Trans.* **2004**, 4193. (b) Leung, W.-P.; Chong, K.-H.; Wu, Y.-S.; So, C.-W.; Chan, H.-S.; Mak, T. C. W. *Eur. J. Inorg. Chem.* **2006**, 808. (c) Leung, W.-P.; Chiu, W.-K.; Chong, K.-H.; Mak, T. C. W. *Chem. Commun.* **2009**, 6822. (d) Zhang, S.-H.; Yeong, X.-H.; So, C.-W. *Chem.—Eur. J.* **2011**, *17*, 3490. (e) Ghadwal, R. S.; Azhakar, R.; Roesky, H. W.; Pröpper, K.; Dittrich, B.; Klein, S.; Frenking, G. *J. Am. Chem. Soc.* **2011**, *133*, 17552. (f) Bouška, M.; Dostál, L.; de Proft, F.; Růžička, A.; Lyčka, A.; Jambor, R. *Chem.—Eur. J.* **2011**, *17*, 455. (g) Ghadwal, R. S.; Azhakar, R.; Roesky, H. W.; Pröpper, K.; Dittrich, B.; Goedecke, C.; Frenking, G. *Chem. Commun.* **2012**, *48*, 8186. (h) Siwatch, R. K.; Nagendran, S. *Organometallics* **2012**, *31*, 3389. (i) Sinhababu, S.; Siwatch, R. K.; Mukherjee, G.; Rajaraman, G.; Nagendran, S. *Inorg. Chem.* **2012**, *51*, 9240. (j) Karwasara, S.; Sharma, M. K.; Tripathi, R.; Nagendran, S. *Organometallics* **2013**, *32*, 3830. (k) Siwatch, R. K.; Yadav, D.; Mukherjee, G.; Rajaraman, G.; Nagendran, S. *Inorg. Chem.* **2013**, *52*, 13384.

(4) Fischer, R. C.; Power, P. P. *Chem. Rev.* **2010**, *110*, 3877.

(5) (a) Li, L.; Fukawa, T.; Matsuo, T.; Hashizume, D.; Fueno, H.; Tanaka, K.; Tamao, K. *Nat. Chem.* **2012**, *4*, 361. (b) Xiong, Y.; Yao, S.; Driess, M. *Angew. Chem., Int. Ed.* **2013**, *52*, 4302.

(6) (a) Kuchta, M. C.; Parkin, G. *J. Chem. Soc., Chem. Commun.* **1994**, 1351. (b) Leung, W.-P.; Kwok, W.-H.; Law, L. T. C.; Zhou, Z.-Y.; Mak, T. C. W. *Chem. Commun.* **1996**, 505. (c) Tokitoh, N.; Matsumoto, T.; Okazaki, R. *J. Am. Chem. Soc.* **1997**, *119*, 2337. (d) Ossig, G.; Meller, A.; Brönneke, C.; Müller, O.; Schäfer, M.; Herbst-Irmer, R. *Organometallics* **1997**, *16*, 2116. (e) Chivers, T.; Eisler, D. J. *Angew. Chem., Int. Ed.* **2004**, *43*, 6686. (f) van Almsick, T.; Kromm, A.; Sheldrick, W. S. *Z. Anorg. Allg. Chem.* **2005**, *631*, 19. (g) Junold, K.; Baus, J. A.; Burschka, C.; Auerhammer, D.; Tacke, R. *Chem.—Eur. J.* **2012**, *18*, 16288.

(7) (a) Dias, H. V. R.; Jin, W.; Ratcliff, R. E. *Inorg. Chem.* **1995**, *34*, 6100. (b) Dias, H. V. R.; Wang, Z. *J. Am. Chem. Soc.* **1997**, *119*, 4650. (c) Dias, H. V. R.; Wang, Z.; Jin, W. *Coord. Chem. Rev.* **1998**, *176*, 67. (d) Siwatch, R. K.; Kundu, S.; Kumar, D.; Nagendran, S. *Organometallics* **2011**, *30*, 1998. (e) Yadav, D.; Siwatch, R. K.; Sinhababu, S.; Nagendran, S. *Inorg. Chem.* **2014**, *53*, 600.

(8) Pauling, L. *The Nature of The Chemical Bond*, 3rd ed.; Cornell University Press: Ithaca, 1960; p 224.

(9) Frisch, M. J.; et al. *Gaussian 09, Revision C. 01*; Gaussian, Inc.: Wallingford, CT, 2010.

(10) Weinhold, F.; Landis, C. R. *Valency and Bonding*; Cambridge: Cambridge, U.K., 2005.

(11) (a) Reed, A. E.; Curtiss, L. A.; Weinhold, F. *Chem. Rev.* **1988**, *88*, 899. (b) Glendening, E. D.; Reed, A. E.; Carpenter, J. E.; Weinhold, F. *NBO, Version 3.1*; Theoretical Chemistry Institute, University of Wisconsin: Madison, WI, 1996.

(12) (a) Glendening, E. D.; Badenhoop, J. K.; Weinhold, F. *J. Comput. Chem.* **1998**, *19*, 628. (b) Glendening, E. D.; Weinhold, F. *J. Comput. Chem.* **1998**, *19*, 610. (c) Glendening, E. D.; Weinhold, F. *J. Comput. Chem.* **1998**, *19*, 593. (d) Glendening, E. D.; Badenhoop, J. K.; Reed, A. E.; Carpenter, J. E.; Bohmann, J. A.; Morales, C. M.; Weinhold, F. *NBO 5.0*; Theoretical Chemistry Institute, University of Wisconsin: Madison, WI, 2001.

(13) Siwatch, R. K.; Nagendran, S. Unpublished results.

(14) Fulmer, G. R.; Miller, A. J. M.; Sherden, N. H.; Gottlieb, H. E.; Nudelman, A.; Stoltz, B. M.; Bercaw, J. E.; Goldberg, K. I. *Organometallics* **2010**, *29*, 2176.

(15) *SMART: Bruker Molecular Analysis Research Tool, Version 5.618*; Bruker AXS: Madison, WI, 2000.

(16) *SAINT-NT, Version 6.04*; Bruker AXS: Madison, WI, 2001.

(17) *SHELXTL-NT, Version 6.10*; Bruker AXS: Madison, WI, 2000.

(18) Spek, A. L. *J. Appl. Crystallogr.* **2003**, *36*, 7.